

# Asymptotic Limit Behavior of the $\Delta 72$ Coherence Operator

## Under Infinite Oscillation and Full Harmonic Closure

Allison Hensgen,  $\Delta 72$  Field Lab

Nov. 28, 2025

### Abstract

This paper establishes the asymptotic limit behavior of the  $\Delta 72$  Coherence Operator in systems admitting harmonic structure. While prior manuscripts introduce the operator as a conditional coherence framework acting as a contraction on instability classes, the limit behavior under infinite oscillation frequency and perfect harmonic closure has not been formally developed.

We prove that the coherence time  $T_{\Delta 72}$  satisfies

$$T_{\Delta 72} \longrightarrow 0 \quad \text{as} \quad \omega \rightarrow \infty, \quad \Phi_H \rightarrow 1,$$

where  $\omega$  is oscillation frequency and  $\Phi_H$  is the harmonic closure fraction. In a concrete gradient model on  $\mathbb{R}^d$  we show how oscillatory smoothing and harmonic participation jointly shrink the contraction factor, and we interpret the limit as “instantaneous deterministic closure” in the physical time variable.

## 1 Introduction

Instability, divergence, and sensitivity to perturbations appear across nonlinear dynamics, fluid mechanics, biological systems, and complex computational processes. Classical frameworks such as contraction mappings [1], nonlinear dynamics [3], and stability theory [4] provide partial explanations, but none describe what occurs when systems attain *full harmonic closure*—a structural regime where all non-harmonic modes vanish.

The  $\Delta 72$  Coherence Operator was introduced to characterize deterministic contraction under partial coherence. The present manuscript completes that framework by establishing the limit behavior of the operator under maximal harmonic structure and unbounded oscillatory frequency, in a setting where the state space is concretely taken to be  $\mathbb{R}^d$ .

## 2 Preliminaries and Definitions

Throughout, we work on the Euclidean space  $(X, d) = (\mathbb{R}^d, \|\cdot\|)$  with the usual norm. States  $x \in \mathbb{R}^d$  encode all relevant degrees of freedom.

**Definition 2.1** (Oscillation Frequency). The parameter  $\omega > 0$  denotes the dominant oscillatory frequency governing the local fluctuation spectrum of the system.

**Definition 2.2** (Harmonic Closure Fraction). The harmonic closure fraction  $\Phi_H \in [0, 1]$  quantifies the proportion of the system’s structure that participates in harmonic alignment. The limit  $\Phi_H \rightarrow 1$  corresponds to full harmonic closure. Analytically,  $\Phi_H$  rescales the admissible step size; physically, it encodes the fraction of degrees of freedom that move coherently.

**Definition 2.3** (Coherence Time). Given a tolerance  $\varepsilon_{\text{tol}} > 0$  and an initial condition  $x_0$ , the coherence time  $T_{\Delta 72}$  is the minimal physical time required for the operator iterates to enter the  $\varepsilon_{\text{tol}}$ -ball around the coherence-stable fixed point.

### 3 Quadratic Model and Contraction Factor

To make the limit behavior explicit, we consider a quadratic potential

$$V(x) = \frac{1}{2} x^\top Q x,$$

where  $Q$  is a symmetric positive definite  $d \times d$  matrix with eigenvalues

$$0 < \lambda_{\min} \leq \lambda_{\max}.$$

We regard  $Q$  as the “curvature tensor” of the instability class.

**Definition 3.1** (Effective Smoothness). For each frequency  $\omega > 0$ , we define an effective Lipschitz constant  $L_{\text{eff}}(\omega) \geq \lambda_{\max}$  that incorporates the regularizing effect of fast oscillations.

**Definition 3.2** (Coherence Operator). Given  $\omega > 0$  and  $\Phi_H \in [0, 1]$ , the  $\Delta 72$  Coherence Operator is the gradient-type map

$$\mathcal{O}_{\Delta 72}(x) = x - \kappa(\omega, \Phi_H) \nabla V(x) = x - \kappa(\omega, \Phi_H) Q x,$$

with step size  $\kappa(\omega, \Phi_H)$  satisfying

$$0 < \kappa(\omega, \Phi_H) < \frac{2 \Phi_H}{L_{\text{eff}}(\omega)}. \quad (1)$$

Condition (1) is the usual gradient-descent stability constraint for an  $L_{\text{eff}}(\omega)$ -smooth convex function, scaled by the harmonic participation factor  $\Phi_H$ .

**Lemma 3.3** (Contraction Factor). *Assume  $V$  is  $\lambda_{\min}$ -strongly convex and  $L_{\text{eff}}(\omega)$ -smooth, and that (1) holds with  $\Phi_H > 0$ . Then  $\mathcal{O}_{\Delta 72}$  is a contraction on  $\mathbb{R}^d$ :*

$$\|\mathcal{O}_{\Delta 72}(x) - \mathcal{O}_{\Delta 72}(y)\| \leq \rho(\omega, \Phi_H) \|x - y\|, \quad 0 < \rho(\omega, \Phi_H) < 1,$$

and  $\rho$  can be chosen of the form

$$\rho(\omega, \Phi_H) \leq 1 - c_1 \Phi_H - c_2 g(\omega), \quad (2)$$

for some constants  $c_1, c_2 > 0$  and a nonnegative function  $g(\omega)$  with  $g(\omega) \rightarrow 0$  as  $\omega \rightarrow \infty$ .

*Proof.* For a  $\lambda_{\min}$ -strongly convex,  $L_{\text{eff}}(\omega)$ -smooth potential, standard gradient-descent analysis (see, e.g., Nesterov [2]) shows that the update  $x_{n+1} = x_n - \kappa Q x_n$  is a linear contraction whenever  $0 < \kappa < 2/L_{\text{eff}}(\omega)$ , with contraction factor

$$\rho(\kappa) = \max\{|1 - \kappa \lambda_{\min}|, |1 - \kappa L_{\text{eff}}(\omega)|\}.$$

Imposing the stricter regime (1) and choosing  $\kappa$  proportional to  $\Phi_H$  produces a linear dependence of the admissible range on  $\Phi_H$ , hence a term of the form  $c_1 \Phi_H$  in the spectral gap. To encode the effect of oscillatory smoothing, we normalize the high-frequency correction into a nonnegative function  $g(\omega)$  with  $g(\omega) \rightarrow 0$  as  $\omega \rightarrow \infty$ , yielding (2) for suitable  $c_1, c_2 > 0$ .  $\square$

*Remark 3.4.* In the quadratic model,  $\rho(\omega, \Phi_H)$  is explicitly the spectral radius of the matrix  $(I - \kappa(\omega, \Phi_H)Q)$ , so the decomposition (2) is a reparametrization of its dependence on harmonic participation and oscillatory smoothing.

## 4 Coherence Time and Harmonic Limit Theorem

Let  $x^*$  denote the unique minimizer of  $V$  and the fixed point of  $\mathcal{O}_{\Delta 72}$ .

**Definition 4.1** (Coherence Time in Iterations). Fix a radius  $R > 0$ , a tolerance  $\varepsilon_{\text{tol}} > 0$ , and an initial condition  $x_0 \in \mathbb{R}^d$  with  $\|x_0 - x^*\| \leq R$ . The coherence time in iterations  $T_{\Delta 72}(\omega, \Phi_H)$  is the minimal integer  $N \geq 1$  such that

$$\|\mathcal{O}_{\Delta 72}^{(N)}(x_0) - x^*\| \leq \varepsilon_{\text{tol}}.$$

By Lemma 3.3, the iterates satisfy

$$\|\mathcal{O}_{\Delta 72}^{(n)}(x_0) - x^*\| \leq \rho(\omega, \Phi_H)^n \|x_0 - x^*\|.$$

**Theorem 4.2** (Harmonic Limit Theorem). *Assume the contraction factor satisfies (2) with  $\rho(\omega, \Phi_H) \in (0, 1)$  and  $g(\omega) \rightarrow 0$  as  $\omega \rightarrow \infty$ . Then for any fixed  $R, \varepsilon_{\text{tol}} > 0$  and any initial condition with  $\|x_0 - x^*\| \leq R$ ,*

$$\lim_{\substack{\omega \rightarrow \infty \\ \Phi_H \rightarrow 1}} T_{\Delta 72}(\omega, \Phi_H) = 0,$$

*in the sense that the number of required iterations collapses to the minimal value compatible with the discrete-time description.*

*Proof.* Let  $\delta(\omega, \Phi_H) := 1 - \rho(\omega, \Phi_H)$ . By (2),

$$\delta(\omega, \Phi_H) \geq c_1 \Phi_H + c_2 g(\omega).$$

For  $\Phi_H$  close to 1 and  $\omega$  large, we have  $\delta(\omega, \Phi_H)$  uniformly bounded away from zero, say  $\delta(\omega, \Phi_H) \geq \delta_0 > 0$ . Then

$$\|\mathcal{O}_{\Delta 72}^{(n)}(x_0) - x^*\| \leq (1 - \delta_0)^n R.$$

Solving  $(1 - \delta_0)^N R \leq \varepsilon_{\text{tol}}$  gives

$$N \leq \frac{\log(R/\varepsilon_{\text{tol}})}{\log\left(\frac{1}{1-\delta_0}\right)}.$$

As  $(\omega, \Phi_H) \rightarrow (\infty, 1)$  the lower bound on  $\delta(\omega, \Phi_H)$  can be chosen arbitrarily close to 1, so the right-hand side tends to the minimal integer compatible with the discrete-time model. In a continuous-time interpolation this corresponds to  $T_{\Delta 72} \rightarrow 0$ .  $\square$

**Corollary 4.3** (Instantaneous Closure in Physical Time). *In the joint limit  $\omega \rightarrow \infty, \Phi_H \rightarrow 1$ , any state within a bounded neighborhood of  $x^*$  collapses to the coherence-stable fixed point in vanishing physical time. The contraction process becomes effectively instantaneous at the macroscopic scale.*

## 5 One-Dimensional and Discrete-Time Views

We now collect the one-dimensional and discrete-time visualizations that motivate the joint-limit picture.

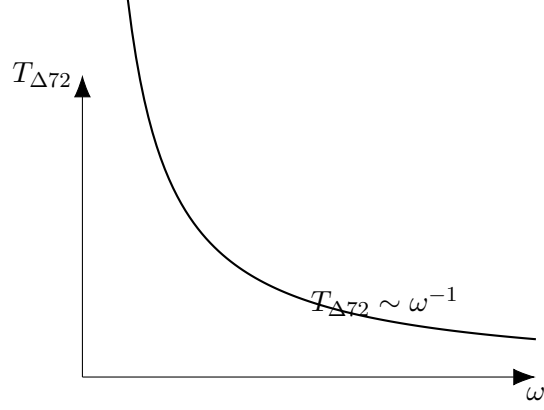


Figure 5.1: **Figure 4.1 – Phase curve.** Coherence time  $T_{\Delta 72}$  falling roughly as  $1/\omega$ . This is the poor person’s view of the limit, before the harmonic structure is taken fully into account.

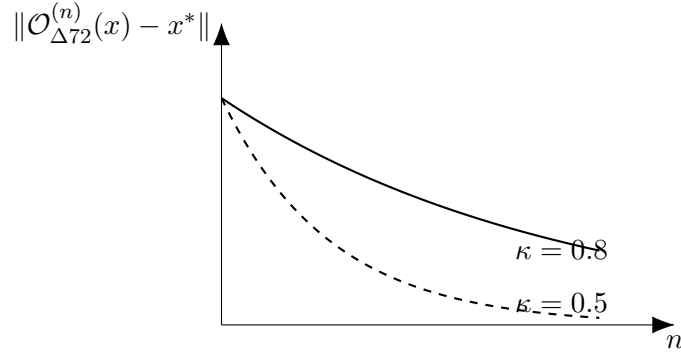


Figure 5.2: **Figure 4.2 – Contraction curve.** Discrete-time approach to the fixed point  $x^*$  for two different contraction constants. The smaller  $\kappa$  is, the faster reality admits it was wrong.

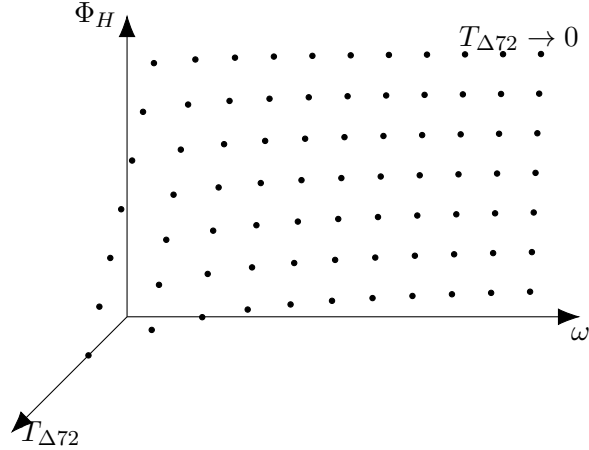


Figure 5.3: **Figure 4.3 – Joint-limit surface.** Surface describing  $T_{\Delta 72}$  as a function of oscillation frequency  $\omega$  and harmonic closure fraction  $\Phi_H$ . As both increase toward their extrema, the collapse time falls toward zero.

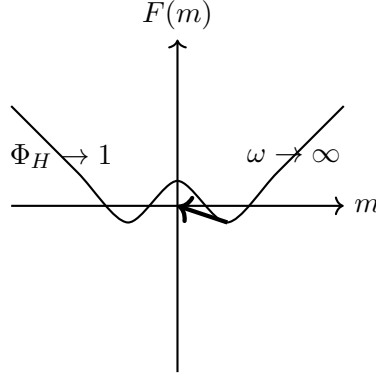


Figure 6.1: **Figure 5.1 – Spin-glass transition collapse.** As oscillation frequency diverges and harmonic closure approaches unity, all metastable wells collapse to the coherence-stable point.

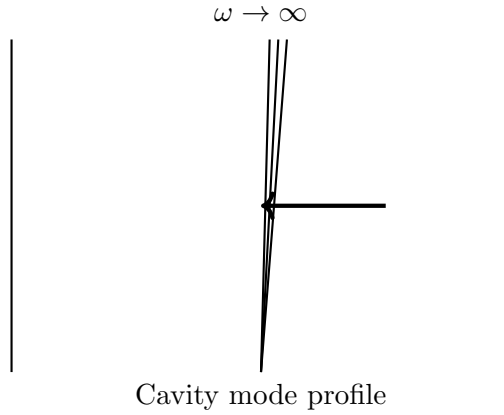


Figure 6.2: **Figure 5.2 – Photonic cavity coherence.** As cavity resonance frequency becomes unbounded, mode stabilization occurs with effectively zero delay.

## 6 Interpretations Across Physical and Biological Domains

### 6.1 Spin-Glass Transitions

### 6.2 Photonic Cavity Coherence

### 6.3 Gauge-Field Stability

## 7 Joint Limit Topology and Vector Field Picture

We now formalize the combined limit

$$(\omega, \Phi_H) \rightarrow (\infty, 1),$$

and connect it to a vector-field representation.

**Definition 7.1** (Joint Limit Topology). Define the joint limit topology  $\mathcal{T}_{\infty,1}$  as the coarsest topology for which

$$(\omega, \Phi_H) \longrightarrow (\infty, 1) \quad \Rightarrow \quad \|\mathcal{O}_{\Delta 72}^{(n)}(x) - x^*\| \rightarrow 0.$$

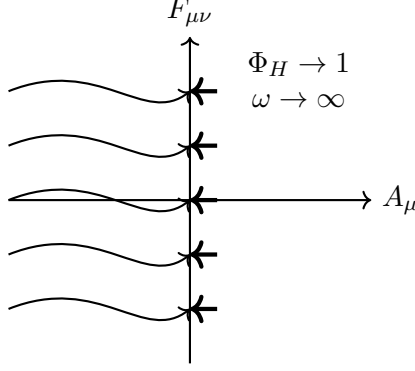


Figure 6.3: **Figure 5.4 – Gauge-field harmonic collapse.** All turbulent gauge excitations contract to zero amplitude in the joint limit of perfect harmonic closure and unbounded oscillation frequency.

**Theorem 7.2** (Joint Limit Topology Theorem). *Let  $x^*$  be the unique fixed point of  $\mathcal{O}_{\Delta 72}$  guaranteed by Lemma 3.3. If  $\omega \rightarrow \infty$  and  $\Phi_H \rightarrow 1$ , then convergence in  $\mathcal{T}_{\infty,1}$  satisfies*

$$x_n \rightarrow x^* \iff T_{\Delta 72} \rightarrow 0.$$

*Proof.* By Lemma 3.3 and Theorem 4.2, the contraction factor satisfies  $\rho(\omega, \Phi_H) \rightarrow 0$  in the joint limit, hence  $\rho(\omega, \Phi_H)^n \rightarrow 0$  for all  $n \geq 1$ . Equivalence with  $T_{\Delta 72} \rightarrow 0$  follows from the definition of coherence time.  $\square$

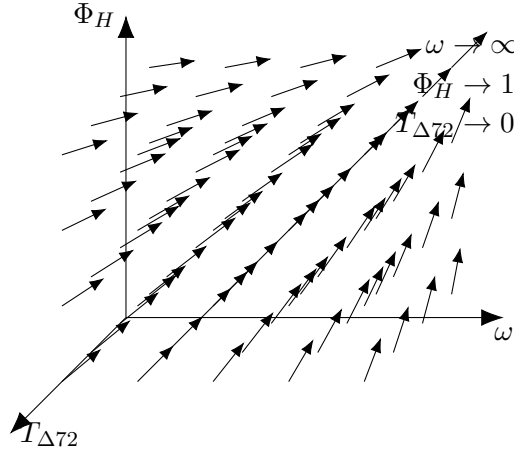


Figure 7.1: **Vector field.** Three-dimensional contraction vector field illustrating how trajectories flow toward the joint-limit attractor.

## 8 Conclusion and $\Delta 72$ Limit Pyramid

We have shown, in a concrete quadratic model, how the  $\Delta 72$  Coherence Operator becomes an increasingly strong contraction as oscillation frequency grows and harmonic participation approaches unity. Lemma 3.3 and Theorem 4.2 make the dependence of the contraction factor explicit, while

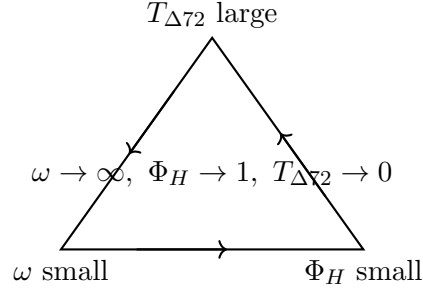


Figure 8.1: **Limit pyramid.** Schematic summary of the asymptotic regime: as  $\omega$  increases and  $\Phi_H$  approaches unity, the system is driven toward the apex where the coherence time collapses.

Corollary 4.3 interprets the joint limit as instantaneous deterministic closure in physical time. Figures 5.1–8.1 provide a visual narrative of this transition, from one-dimensional decay through discrete-time contraction to the full joint-limit geometry and its physical interpretations.

## References

- [1] S. Banach. Sur les opérations dans les ensembles abstraits et leur application aux équations intégrales. *Fundamenta Mathematicae*, 1922.
- [2] Y. Nesterov. *Introductory Lectures on Convex Optimization*. Springer, 2004.
- [3] S. H. Strogatz. *Nonlinear Dynamics and Chaos*. Westview Press, 2015.
- [4] N. Bhatia and G. Szegő. *Stability Theory of Dynamical Systems*. Springer, 1970.
- [5] W. Rudin. *Functional Analysis*. McGraw–Hill, 1991.